Title

The differential regulation of placenta trophoblast bisphosphoglycerate mutase in fetal growth restriction: preclinical study in mice and observational histological study of human placenta.

Authors

Sima Stroganov[1], Talia Harris[2], Liat Fellus-Alyagor[3], Lital Ben Moyal[1], Romina Plitman Mayo[1], Ofra Golani[4], Hirsch Dana[3], Shifra Ben-Dor[4], Alexander Brandis[4], Tevie Mehlman[4], Michal Kovo[5], Tal Biron-Shental[5], Nava Dekel[1], Michal Neeman[1]

1. Immunology and Regenerative Biology, Weizmann Institute of Science, Rehovot, Israel

2. Chemical Research Support Weizmann Institute of Science, Rehovot, Israel

3. Veterinary Resources, Weizmann Institute of Science, Rehovot, Israel

4. Life Science Core Facilities, Weizmann Institute of Science, Rehovot, Israel

5 OBGYN, Meir Medical Center, Kfar Saba; Tel Aviv University, School of Medicine, Israel

Abstract

Background Fetal growth restriction (FGR) is a pregnancy complication in which a newborn fails to achieve its growth potential, increasing the risk of perinatal morbidity and mortality. Chronic maternal gestational hypoxia, as well as placental insufficiency are associated with increased FGR incidence; however, the molecular mechanisms underlying FGR remain unknown.

Methods Pregnant mice were subjected to acute or chronic hypoxia (12.5% O_2) resulting in reduced fetal weight. Placenta oxygen transport was assessed by blood oxygenation level dependent (BOLD) contrast magnetic resonance imaging (MRI). The placentae were analyzed via immunohistochemistry and in situ hybridization. Human placentae were selected from FGR and matched controls and analyzed by immunohistochemistry (IHC). Maternal and cord sera were analyzed by mass spectrometry.

Results We show that murine acute and chronic gestational hypoxia recapitulates FGR phenotype and affects placental structure and morphology. Gestational hypoxia decreased labyrinth area, increased the incidence of red blood cells (RBCs) in the labyrinth while expanding the placental spiral arteries (SpA) diameter. Hypoxic placentae exhibited higher hemoglobin-oxygen affinity compared to the control. Placental abundance of Bisphosphoglycerate mutase (BPGM) was upregulated in the syncytiotrophoblast and spiral artery trophoblast cells (SpA TGCs) in the murine gestational hypoxia groups compared to the control. Hif1a levels were higher in the acute hypoxia group compared to the control. In contrast, human FGR placentae exhibited reduced BPGM levels in the syncytiotrophoblast layer compared to placentae from healthy uncomplicated pregnancies. Levels of 2,3 BPG, the product of BPGM, were lower in cord serum of human FGR placentae compared to control. Polar expression of BPGM, was found in both human and mouse placentae syncytiotrophoblast, with higher expression facing the maternal circulation. Moreover, in the murine SpA TGCs expression of BPGM was concentrated exclusively in the apical cell side, in direct proximity to the maternal circulation.

Conclusions This study suggests a possible involvement of placental BPGM in maternal-fetal oxygen transfer, and in the pathophysiology of FGR.

Funding This work was supported by the Weizmann Krenter Foundation and the Weizmann – Ichilov (Tel Aviv Sourasky Medical Center) Collaborative Grant in Biomedical Research, and by the Minerva Foundation (to MN), by the ISF KillCorona grant 3777/19 (to MN, MK).

Introduction

The placenta is a transient organ, crucial for the growth and development of the fetus during gestation[12]. The placenta provides the interface between the maternal and fetal circulation, mediating gas and metabolic exchange along with fetal waste disposal[3]. Abnormalities in placental growth, structure, and function are associated with gestational complications such as fetal growth restriction (FGR)[45], which is defined as the failure of the fetus to reach its growth potential[6]. The clinical definition of FGR is fetal weight below the 10th percentile of predicted fetal weight for gestational age[7]. FGR affects approximately 10-15% of pregnancies, increasing the risk of perinatal morbidity and mortality[6]. Long-term complications of FGR include poor

57 postnatal development and are associated with multiple adverse health outcomes including
58 respiratory, metabolic and cardiovascular deficits [89].

59 There are numerous etiologies for FGR, some of which are related to fetal genetic aberrations or
60 malformations, others related to placental or umbilical malformation, or also to maternal
61 infections or diseases. Maternal anemia, smoking, high altitude residency, as well as placental
62 and umbilical cord anomalies, are all associated with restricted placental and fetal oxygen
63 availability[10]. Interestingly, about 40 percent of all FGR cases are idiopathic[11], with no
64 identifiable cause, which might hint on possible biological pre disposition factors that contribute
65 to FGR development by creating an hypoxic placental or embryo environment. However, the
66 molecular mechanisms that provoke and contribute to this pregnancy complication have yet to
67 be elucidated.

68 One of the key placental functions is the transfer of oxygen from the mother to the fetus[12], and
69 inefficient oxygen transport and availability is detrimental for placental and embryonic
70 development[1314]. Late-gestation hypoxia results in utero-placental vascular adaptations, such as
71 capillary expansion, thinning of the inter-haemal membrane and increased radial artery
72 diameters[15]. Moreover, there is substantial evidence that late-gestation exposure to hypoxic
73 environment alters placental structure and functionality[1617]. *In-vitro* studies on human placental
74 samples under acute reduction of oxygen tension induced direct placental vasoconstriction[18].
75 Placental oxygen transport depends on Hemoglobin (Hb), which is responsible for carrying and
76 mediating oxygen transfer in mammalian organisms[19]. BOLD contrast MR imaging is a powerful
77 tool that utilizes hemoglobin as an endogenous reporter molecule to assess oxygen-hemoglobin
78 affinity[20]. Previous MR studies have shown altered placental oxygen-Hb affinity following
79 exposure to hypoxia[21]. However, limited information is available on how placental structure and
80 function is altered in chronic gestational hypoxia that commences at the onset of gestation.

81 The most significant allosteric effectors of Hb are organic phosphates, specifically 2,3 BPG,
82 which is produced by the BPGM enzyme in a unique side reaction of glycolysis, known as the
83 Luebering-Rapoport pathway[22]. 2,3 BPG plays a key role in delivering O_2 to tissues by binding to
84 and stabilizing deoxy-hemoglobin, thus leading to the release of oxygen from the Hb unit[2324].
85 During gestation, fetal hemoglobin (HbF) is the dominant form of Hb present in the fetus,
86 comprised of α and γ subunits[25]. During late gestation, the γ subunit is gradually replaced by the
87 adult β subunit[25]. HbF has a higher affinity to oxygen compared to the adult Hb, caused by a

88 structural difference, which leads to a weakened ability to bind 2,3 BPG[262728]. The transfer of
89 oxygen from maternal to fetal Hb is facilitated by the higher affinity of maternal Hb to 2,3 BPG[24].
90 Remarkably, BPGM expression is specifically restricted to erythrocytes and the
91 syncytiotrophoblast of the placenta, a multinucleated layer that mediates transport of oxygen
92 and nutrients from the mother to the fetus[29]. In a study that used *Igf2*$^{+/-}$ knockout mice as a
93 model of FGR, BPGM expression in the placental labyrinth was lower compared to wild type
94 placentae[30]. However, scarce information is available on the role of this enzyme during
95 gestation. We report here that placental BPGM expression pattern is consistent with a role in
96 adaptation of the placenta to gestational hypoxia, facilitating the transfer of oxygen from
97 maternal to fetal circulation. Here we show that gestational hypoxia augments placental BPGM
98 expression in mice, while in human FGR placentae of unknown etiology BPGM expression is
99 suppressed.

100

101 **Methods**

102 **Animals**

103 Female C57BL/6JOlaHsd mice (8-12 weeks old; Envigo, Jerusalem; n=28) were mated with
104 C57BL/6JOlaHsd male mice (Envigo, Jerusalem; n=8). Detection of a vaginal plug the following
105 day was considered embryonic day 0.5 (E0.5). At E0.5 or E11.5, the pregnant females were
106 randomly allocated to control (21% O_2, n = 15) or hypoxia group (12.5% O_2, acute hypoxia; n=6,
107 chronic hypoxia; n=7). Throughout the experiments, the animals were maintained in a
108 temperature-controlled room (22 ± 1°C) on a 12h:12h light–dark cycle. Food and water was
109 provided *ad libitum* and animal well-being was monitored daily. At E16.5 the pregnant females
110 were analyzed using high-field MRI under a respiration challenge of hyperoxia-to-hypoxia (40%
111 O_2, 20% O_2, 10% O_2). After MR imaging, the animals were sacrificed via cervical dislocation for
112 tissue collection. All experimental protocols were approved by the Institutional Animal Care and
113 Use Committee (IACUC) of the Weizmann Institute of Science, Protocol number: 07341021-2.

114 **Establishment of Maternal Hypoxia Models**

115 We applied two models of maternal hypoxia – acute and chronic. The pregnant mice were
116 housed in a hypoxic chamber (VelO2x, Baker Ruskinn, Sanford, Maine, USA) from E11.5 (acute
117 hypoxia; n=6) or E0.5 (chronic hypoxia; n=7) until E16.5. On the first day in the hypoxic chamber,

118 maternal oxygen supply was gradually reduced from 21%O_2 to 12.5 ± 0.2% O_2 by continuous
119 infusion of a nitrogen gas. The water contained in the expired gas was trapped using silica gel
120 beads (Merck, CAS #: 7631-86-9). A portable oxygen analyzer (PO_2-250, Lutron, Coopersburg,
121 Pennsylvania, United States) was used to monitor the oxygen concentration in the chamber.
122 Pregnant control females were housed in an identical chamber supplied with a constant 21% ±
123 0.2% O_2 concentration.

124 ***In Vivo* MR Imaging**

125 MR imaging examinations were performed at a 15.2T with an MR spectrometer (BioSpec 152/11
126 US/R; Bruker, Karlsruhe, Germany) equipped with a gradient-coil system capable of producing
127 pulsed gradients of 10 mT/cm in each of the three orthogonal directions. A quadrature volume
128 coil with a 35-mm inner diameter and an homogeneous radiofrequency field of 30 mm along the
129 axis of the magnetic field was used for both transmission and reception. Immediately prior to
130 MR imaging, the pregnant females were anesthetized with isoflurane (3% for induction; Piramal,
131 Mumbai, India) mixed with 2 L/min of 40% O_2 and 60% N_2 delivered into a closed induction
132 chamber. Once anesthetized, the animals were placed in a prone position in a head holder with
133 breathing gas mixed with isoflurane delivered through a tooth bar. Respiration rate and rectal
134 temperature were monitored using a monitoring and gating system (Model 1030-S-50; SA
135 Instruments, Stony Brook, NY). Respiration rate was maintained throughout the experimental
136 period at approximately 20-30 breaths per minute by adjusting the isoflurane level (1%–2% for
137 maintenance). Body temperature was maintained at 30±1°C (to reduce fetal movement) by
138 adjusting the temperature of a circulating water heating blanket placed above the animal.

139 **MR Imaging Data Acquisition**

140 Anatomic data to determine optimal animal positioning was acquired by using a short Gradient
141 Recalled Echo (GRE) sequence with imaging slices acquired in three orthogonal planes. The
142 animals were positioned to maximize the number of fetuses that could be viewed while still
143 observing maternal liver. The duration of the MRI measurements at each oxygen level was
144 approximately 20 min. After the O_2 concentration was reduced, a 2 minute interval was given
145 before acquiring the next set of MRI images, allowing relaxation rate (R2*) stabilization. At each
146 oxygen phase, the nitrogen level was adjusted to maintain a constant flow of inhaled gas. To
147 determine R2* values three Gradient Recalled Echo (GRE) acquisitions were performed with TE=

148 1.6 ms, 2.6 ms and 3.6 ms. The parameters for these GRE measurements were as follows: 48
149 slices with slice thickness of 0.4 mm with 0.1 mm inter-slice gap, field of view 4.2 X 3.3 cm^2,
150 pulse flip angle 40°, matrix size 280 x 220 (150 x 150 um^2 pixel size), 2 averages (motion
151 averaging). Images were acquired with fat suppression and RF spoiling. The excitation pulse was
152 0.5 ms (6400 Hz bandwidth) and the acquisition bandwidth was 200 kHz. The slice order was
153 interleaved. The sequence was respiration triggered (per slice) with an approximate TR of 800
154 ms.

155 **MR Imaging Data Analysis**

156 Images were reconstructed by Paravision 6.0 (Bruker, Karlsruhe, Germany). The GRE images
157 used for calculating R2*s were interpolated in Matlab (MathWorks, Natick, Massachusetts, USA)
158 to 75X75 um^2 pixel size. Regions of Interest (ROIs) were manually marked with ImageJ (U. S.
159 National Institutes of Health, Bethesda, Maryland, USA). Subsequently, using custom written
160 scripts all ROIs and images were imported into Matlab and the R2* for each O_2 level was
161 determined by fitting the changes in the median signal intensity of each ROI to a single
162 exponential decay [Eq 1]:

163 $Int = Int_0 \cdot e^{-R_2^* \cdot TE}$ [Equation 1]

164 **Tissue collection**

165 Mouse placentae samples: After MR Imaging of the animals, maternal blood was collected from
166 the submandibular vein, followed by cervical dislocation. Maternal hematocrit, Hb and pH levels
167 were determined using i-STAT CG8+ cartridge (Abbott, Cat. No. ABAXIS-600-9001-10, Chicago,
168 Illinois, USA). Uterine tissues were immersed in PBS to count the number of fetuses and
169 resorptions. Fetuses and placentae were immediately removed and weighed, following by
170 fixation in 4% paraformaldehyde. Grade of embryonic and placental weight was classified as SGA
171 (weight less than the 10th percentile), large for gestational age (LGA, weight greater than the
172 90th percentile), and appropriate for gestational age (AGA, weight between the 10th and 90th
173 percentiles).

174 Human placentae samples: The study was approved by the Meir and Wolfson Medical Center
175 IRB Local Committee (Protocols: # 0147-20 MMC and #185-19-WOMC). Written informed
176 consent was obtained from all participants prior to delivery. Placentae from 9 healthy
177 uncomplicated pregnancies and from 7 pregnancies complicated by fetal growth restriction

178 (FGR) were collected immediately after elective cesarean deliveries. Two biopsies were taken
179 from each placenta, one from a peripheral and one from a central lobule. The biopsied material
180 (~ 1 cm^3) was immediately fixed in formalin. FGR birth weight standards were based on the
181 Dollberg curve.

182 Human Serum: Maternal and cord serum samples were collected from the enrolled patients
183 prior to delivery, and from the umbilical cord just following delivery. The umbilical cord was
184 wiped clean and blood was drawn from the vein. Blood samples were centrifuged (1000g, 10
185 minutes at room temperature), and serum aliquots were stored at –80°C in dedicated tubes for
186 analyses at the Weizmann Institute. We used the CDC hemolysis reference palette to exclude
187 the hemolysed samples.

188 **Immunohistochemistry and Microscopy**

189 Fixed murine and human placentae were processed and embedded in paraffin. Representative 5
190 µm sections were taken from each tissue and used for IHC.

191 All slides were dewaxed and rehydrated in xylene and a series of ethanol washes. IHC staining
192 involved antigen retrieval in a pressure cooker using citrate buffer (pH=6) and blocking of non-
193 specific binding with 20% NHS and 0.2% Triton in PBS. Slides were incubated with polyclonal
194 rabbit primary anti-BPGM antibody (1:200, Sigma-Aldrich, Cat. No. HPA016493, RRID:
195 AB_1845414), followed by incubation with an HRP anti-Rabbit secondary antibody (1:100,
196 Jackson ImmunoResearch Labs, Cat# 111-035-003, RRID: AB_2313567) followed by Opal 690
197 (1:500, Akoya Biosciences, Cat. No. FP1497001KT). Negative controls for each immunostaining
198 were incubated with secondary antibody only.

199 Images were captured using Nikon Eclipse Ti2_E microscope, Yokogawa CSU W1 spinning disk,
200 photometrics Prime 25B camera with NIS elements AR 5.11.01 64bit software.

201 For co-detection of BPGM with SynI, SynII, HIf1a and Hif2a, HCR™ IF + HCR™ RNA-FISH protocol
202 for FFPE sections was employed (Molecular Instruments; Schwarzkopf et al., 2021) according to
203 manufacturer instructions using an antibody for BPGM (cat num, company, 1:50, antigen
204 retrieval with PH=6 citric acid), along with probes designed for SynI, SynII, Hif1a and Hif2a.
205 Imaging was done using a Dragonfly spinning disc (Andor, Oxford instruments) on a DMi8
206 microscope (Leica Microsystems) equipped with a Zyla 4.2 camera and a 63C glycerol objective.

207 **Placental Morphological Analysis**

208 For the assessment of placental labyrinth size, fractional area expressing both BPGM and
209 containing fetal RBCs of each placenta was computed *via* use of the color thresholding and area
210 fraction tools in ImageJ. Approximately 10 measurements were made per each placenta. Spiral
211 arteries diameter was measured manually using ImageJ, namely, for each spiral artery 5-6
212 measurements were made. For the assessment of RBC levels in the labyrinth, thresholding of
213 the RBC auto fluorescence signal was employed. Quantification of mouse placental BPGM in the
214 labyrinth was performed using color thresholding in ImageJ, 10 identical measurements were
215 done for each placenta, 500x500 µm each. For the assessment of BPGM in the SpA TGCs, regions
216 of interest were drawn manually implying the same thickness from the inner vessel border
217 followed by color thresholding in ImageJ. We quantified human BPGM expression level by
218 creating a binned intensity histogram of all the pixels expressing BPGM signal above a minimal
219 background value (of 1000), in a single slice of each sample using Fiji Macro[38]. As red blood cells
220 (RBC) have high auto fluorescence in all channels, we discarded RBC regions them prior BPGM
221 quantification. This is done in Imaris (Oxford company) by creating Surface object for RBC
222 (default parameters, automated absolute intensity threshold), and using it to create new PBGM
223 channel in which the values in the RBC regions are set to zero.

224 **BPGM Promoter Analysis**

225 Genomic DNA of the putative promoter regions (~2000 bp upstream, 1000bp downstream of
226 the Transcription Start Site, stopped at genomic repeats on either side) was taken for analysis in
227 GGA (Genomatix Genome Analyzer) MatInspector[39] with the V$HIFF family (Hypoxia inducible
228 factor, bHLH/PAS protein family) matrices (Matrix Family Library Version 11.4, January 2022).

229 **LC–MS/MS measurement of 2,3-BPG**

230 Ten-uL aliquots of plasma were extracted with 80uL of extraction buffer (10mM ammonium
231 acetate/5mM ammonium bicarbonate, pH 7.7 and methanol in ratio 1:3 by volume), and 10uL
232 of methionine sulfone (1ug/mL in water) was added as internal standard. The mixture was
233 vortexed, incubated at 10°C for 10min, then centrifuged (21,000g for 10min). The supernatant
234 was collected for consequent LC–MS/MS analysis. The LC–MS/MS instrument consisting of an
235 Acquity I-class UPLC system (Waters) and Xevo TQ-S triple quadrupole mass spectrometer
236 (Waters), equipped with an electrospray ion source, was used for analysis of 2,3-BPG. MassLynx

237 and TargetLynx software (v.4.1, Waters) were applied for the acquisition and analysis of data.
238 Chromatographic separation was performed on a 150mm × 2.1mm internal diameter, 1.7-µm
239 BEH Z-HILIC column (Waters Atlantis Premier) with mobile phases A (20mM ammonium
240 carbonate, pH 9.25/acetonitrile, 80/20 by volume) and B (acetonitrile) at a flow rate of
241 0.4ml min−1 and column temperature of 25°C. A gradient was used as follows: for 0–0.8min a
242 linear decrease from 80 to 35%B, for 0.8–5.6min further decrease to 25%B, for 5.6–6.0min hold
243 on 25%B, then for 6.0-6.4min back to 80%B, and equilibration at 80%B for 2.6min. Samples kept
244 at 8°C were automatically injected in a volume of 5µl. 2,3-BPG concentration was calculated
245 using a standard curve, ranging from 0.1–100µg ml−1. For MS detection MRM transitions
246 265.0>78.8, 265.0>167.0 m/z (ESI -) were applied in case of 2,3-BPG, with collision energies 31
247 and 12eV, respectively. Internal standard was detected using MRM 182.1>56.0 m/z (ESI +), with
248 collision energy 18eV.

249 **Statistical Analysis**

250 Ordinary one-way Anova test was applied for the comparison between the three pregnant
251 females' groups (control, acute and chronic hypoxia) followed by a Tukey's multiple comparisons
252 test. Litter means were used for statistical analysis of fetal and placental weights. Unpaired *t*-
253 test was used for the analysis of the IF images of FGR and control human placentae. The data
254 were considered to indicate a significant difference when *P* values were less than 0.05. All
255 results are represented as the mean ± SD. Statistical analysis was performed using Graphpad
256 Prism 6 (GraphPad Software, San Diego, USA) for Windows.

257

258 **Results**

259 **Gestational Hypoxia Affects Maternal Hematological Parameters and Recapitulates FGR**
260 **Phenotype**

261 Maternal hypoxia during pregnancy increases the risk of FGR [31,32]. To gain an understanding of
262 BPGM contribution to placental development and functionality following maternal hypoxia, we
263 established a murine model of acute (12.5% O_2, E11.5-E16.5) and chronic gestational hypoxia
264 (12.5% O_2, E0.5-E16.5). Increased erythropoiesis is the best-known physiological response to
265 chronic hypoxia[33]. Exposure to chronic hypoxia during gestation significantly elevated maternal
266 blood hematocrit and Hb levels (by 4.9±1.62 %PCV, *P*=0.0243 and by 1.693±0.54 g/DL, *P*=0.0217

267 respectively, Figure 1 A, B) relative to the control group. Both acute and chronic gestational
268 hypoxia resulted in a significant increase in blood acidity, presented by a decrease in pH values
269 (*P*=0.0032 acute hypoxia versus control, *P*=0.0462 chronic hypoxia versus control, Figure 1 C).

270 Gestational acute and chronic hypoxia did not affect litter size (Figure 1 D). Thereafter, the
271 effect of gestational hypoxia on placental and fetal weight was assessed. A significant decrease
272 in placental weight was observed in both gestational hypoxia groups and in fetuses of the
273 chronic hypoxia group (acute hypoxia placentae by 15.03±4.2 mg, *P*=0.0068, chronic hypoxia
274 placentae by 11.84±4.06 mg, *P*=0.0258 and fetuses by 50.24±18.11 mg, *P*=0.0343, Figure 1 E- G)
275 when compared to the control group. To further examine the weight differences, the percent of
276 small, average or large for gestational age (SGA – small for gestational age, weight less than the
277 10th percentile, AGA - appropriate for gestational age, weight between the 10th and 90th
278 percentiles, LGA - large for gestational age, weight greater than the 90th percentile) fetuses and
279 placentae were compared to the control group. The results show that in the acute hypoxia
280 group 45% of the fetuses are SGA and only 2% LGA, whereas in the chronic hypoxia group 50%
281 of the fetuses are SGA and only 5% LGA (Figure 1 H). Furthermore, the placentae exhibited a
282 similar phenotype, where in the acute hypoxia group 35% of the placentae are SGA and none
283 were LGA, whereas in the chronic hypoxia group 21% of the placentae were SGA and only 1.6%
284 LGA (Figure 1 I).

285

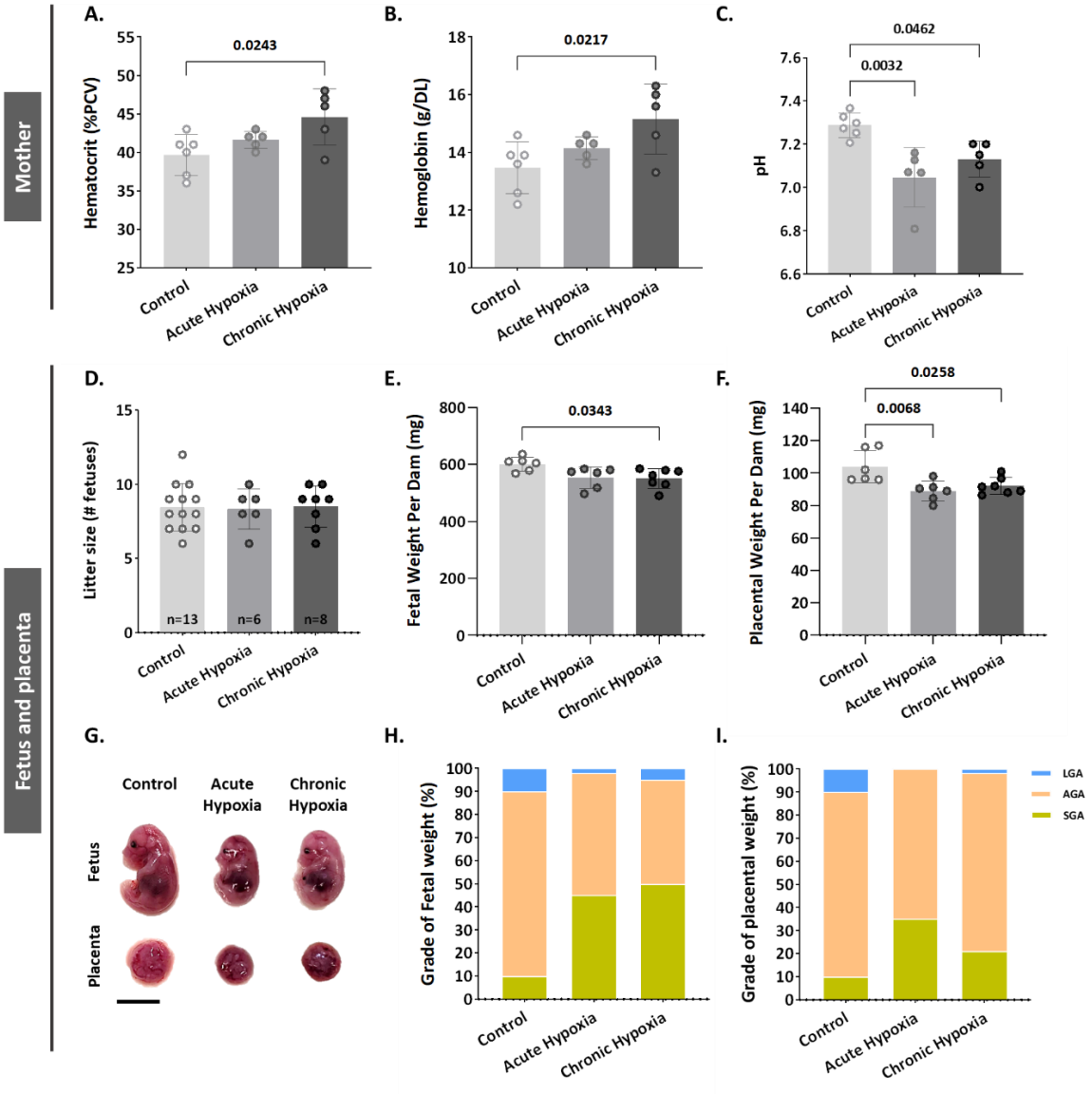

Figure 1. Gestational hypoxia elevates maternal hemoglobin, hematocrit and blood acidity, and recapitulates FGR phenotype in mice. (**A-B**) Graphs showing hematocrit and hemoglobin levels in maternal venous blood. (**C**) Graph shows pH levels in maternal venous blood. (**D-F**) Graphs showing litter size, fetal weight and placental weight. (**G**) Representative picture of fetuses and placentae (E16.5) from control and gestational hypoxia groups. (**H-I**) Analysis of the percentage of small for gestational age (SGA, weight less than the 10th percentile) fetuses and placentae, large for gestational age (LGA, weight greater than the 90th percentile) fetuses and placentae, and appropriate for gestational age (AGA, weight between the 10th and 90th percentiles) fetuses and placentae at E16.5. Scale bars: 1 cm. Data displayed as mean ± SD and are from 49-62 fetuses and placentae from 6-7 dams per group (8–9 conceptuses per litter used). Ordinary one-way ANOVA test was used for statistical analysis.

Gestational Hypoxia Alters Placental Morphology

To determine whether the gestational hypoxia leads to structural changes of the placenta, the placental morphology, and particularly the labyrinth area was examined. The labyrinth area of the chronic and gestational hypoxia-exposed mice was significantly smaller (*P*=0.0001 for the acute and *P*=0.0003 for the chronic hypoxia groups, Figure 2 A, B) compared to the control group. Furthermore, the diameter of the placental spiral arteries (SpA) was enlarged in the chronic hypoxia group (Figure 2 C, D, *P*=0.0420) as compared to the control. In addition, in both acute and chronic hypoxia groups the density of RBCs in the labyrinth were significantly higher (*P*=0.0008 for the acute and *P*=0.007 for the chronic hypoxia groups, Figure 2 E, F) compared to the control.

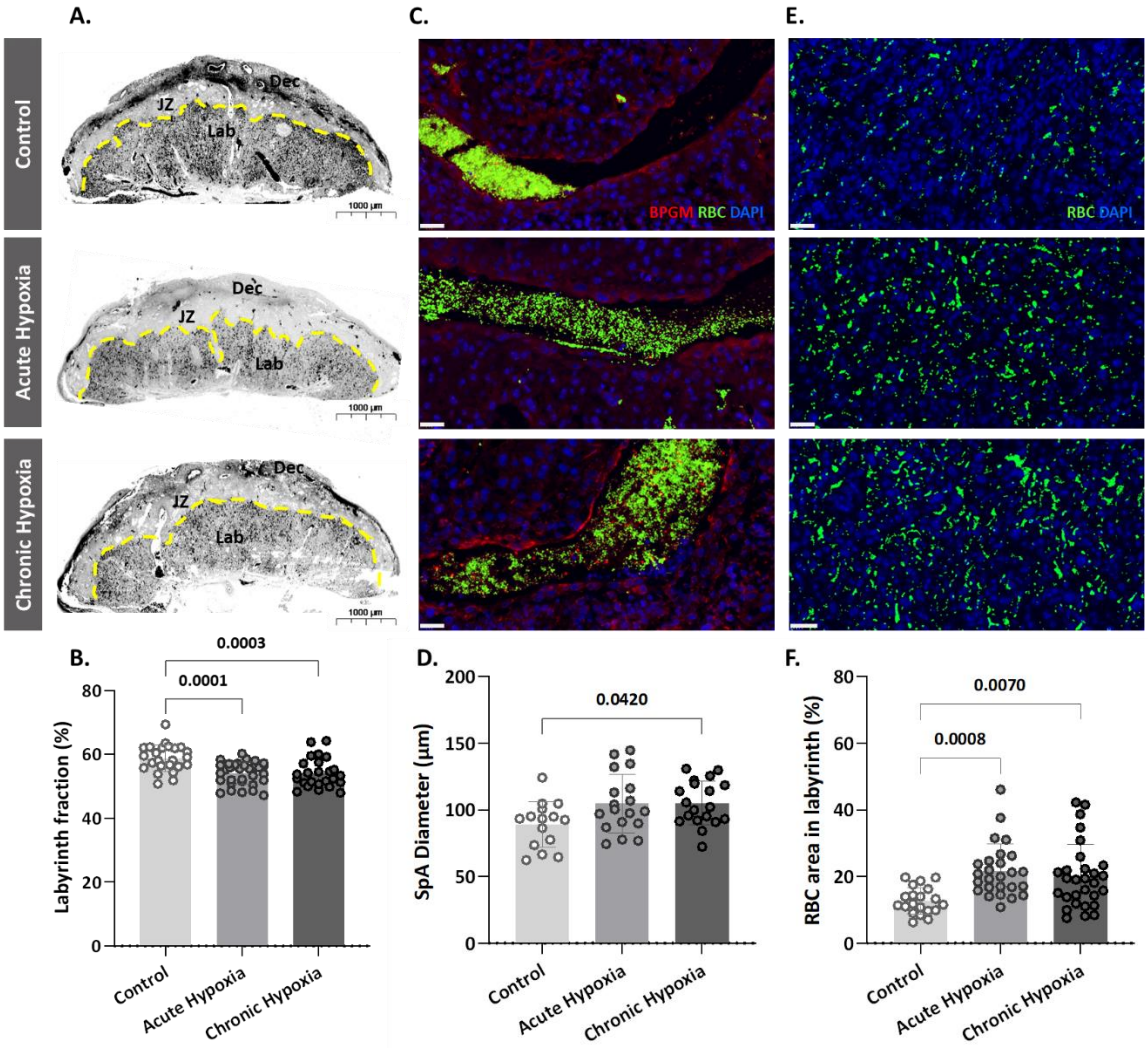

311 **Figure 2. Maternal hypoxia during gestation results in enlarged spiral arteries, increased RBC**
312 **levels and decreased placental labyrinth area.** (**A, B**) Placentae of hypoxic chamber groups have
313 significantly smaller labyrinth area in comparison to the control group. (**C ,D, E, F**) Placentae of
314 hypoxic chamber groups display enlarged spiral arteries and increased RBC levels in the
315 labyrinth. Scale bars: 40 µm. Data are from 3 control, 4 chronic hypoxia and 4 acute hypoxia
316 dams, 5-7 placentae per dam and presented as mean ± SD values. Ordinary one-way ANOVA test
317 was used for statistical analysis.

318

319 **R2* Maps Reveals Maternal, But Not Placental or Fetal changes in deoxygenated hemoglobin**
320 **concentration**

321 As shown above, gestational hypoxia alters placental structure. To determine whether and how
322 gestational hypoxia affects placental functionality, the pregnant dams (E16.5) were subjected to
323 hyperoxia-hypoxia challenge during ultra-high field (15.2T) MR imaging (Figure 3 supplementary
324 video 1, 2, 3). R2* values were calculated at each oxygen challenge for the maternal aorta, vena
325 cava and liver (Figure 3 A-D, Figure 3 Figure supplement 1), and for the placenta, embryo heart,
326 liver and aorta (Figure 3 E-H). The maternal aorta R2* levels from the chronic hypoxia group
327 were significantly higher (P=0.0376, Figure 3 A) than in the control group, when subjected to
328 10% O_2. However, no differences were observed in maternal liver and vena cava when
329 compared to that of the control group (Figure 3 B, D). Similarly, no differences were observed in
330 the R2* of embryonic tissues (aorta, heart and liver), nor in the placenta, when comparing the
331 hypoxic groups to the control (Figure 3 E-H). To better understand the signal distribution in the
332 different placental regions, the R2* maps of the placentae were further analyzed. Interestingly
333 no significant differences in the spatial distribution of R2* were observed in the placentae of
334 hypoxic and control groups (Figure 3 J).

335

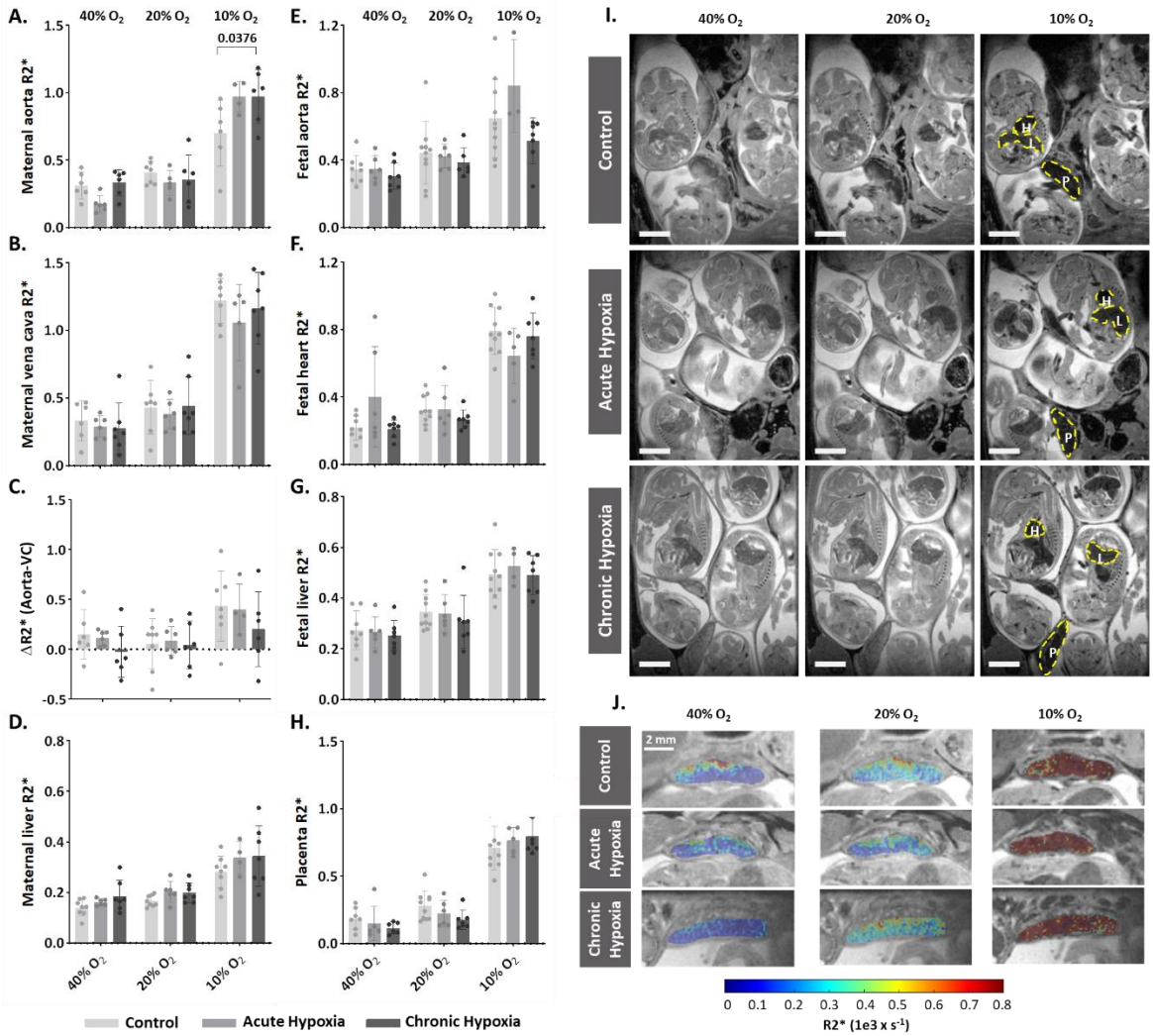

Figure 3. Effects of maternal hypoxia during gestation on R2* values following hyperoxia-hypoxia challenge. (**A-H**) Graphs show that hypoxic challenge results in elevation in R2* values in maternal aortas of chronic hypoxia chamber group, while no differences are observed in the respective placentae and fetuses. (**I**) Representative R2* images of control and hypoxic chamber group show several fetuses and their placenta (P), heart (H) and liver (L). Scale bars: 0.5 cm. (**J**) Representative R2* maps inside the placenta of control, acute hypoxia (AH) and chronic hypoxia (CH) chamber groups at E16.5 show distribution of R2* values following hyperoxia-hypoxia challenge. Data are from 8 control, 6 acute hypoxia and 7 chronic hypoxia per dams presented as mean ± SD values. R2* values of embryonic tissues and placentae are calculated as the median per mother, 5-8 embryos per each mother. Ordinary one-way ANOVA test was used for statistical analysis.

BPGM is Upregulated in Placental Cells Following Gestational Hypoxia

350 Our present findings revealed structural changes in placentae from hypoxic mothers, however
351 functional MRI experiments demonstrated that placental deoxyhemoglobin concentrations are
352 similar to the control group. BPGM expression was previously observed in human placental
353 syncytiotrophoblast cells from healthy pregnancies[29]. Therefore, we inspected the expression of
354 BPGM in the labyrinth of the gestational hypoxia FGR murine model compared to the control
355 (Figure 4, Figure 4 Figure supplement 1, Figure 4 Figure supplement 2).

356 We demonstrate that Bpgm expression is co-localized with both SynI and SynII, the two layers of
357 syncytiotrophoblast in the murine placenta (Figure 4 A). Significant differences were observed in
358 the syncytiotrophoblast BPGM expression between the hypoxic and control placentae (Figure 4
359 B, E). Although BPGM expression has only been reported in the syncytiotrophoblast, we also
360 inspected the BPGM expression in other placental cells that come in direct contact with
361 maternal blood. BPGM expression was found also in the spiral artery trophoblast cells (SpA
362 TGCs), an expression that is upregulated following acute and chronic maternal hypoxia (Figure C,
363 F); moreover, SpA TGCs BPGM expression was found to be polar and concentrated in the apical
364 cell side facing the arterial lumen (Figure 4 D).

365

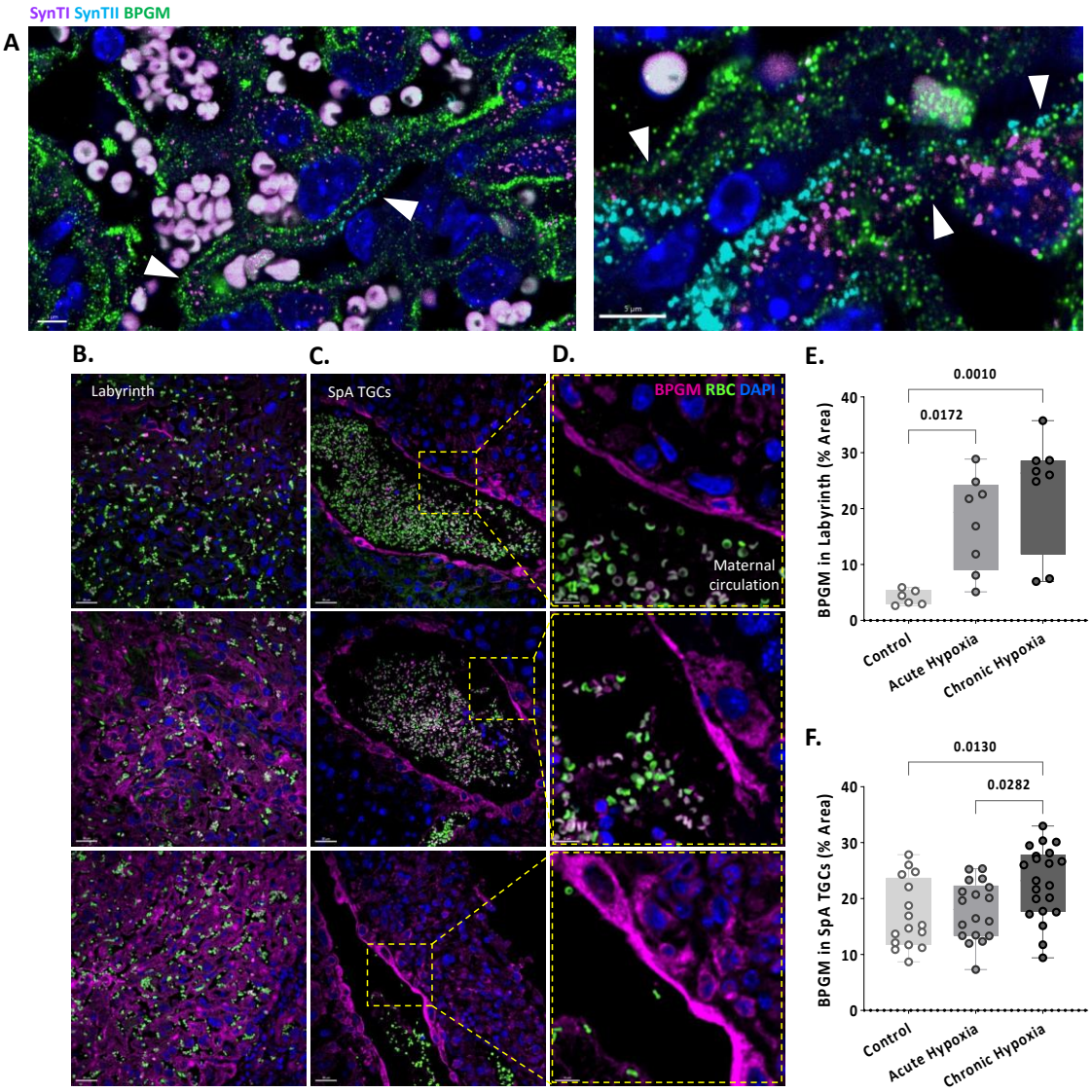

Figure 4. Maternal hypoxia during gestation results in elevated placental BPGM expression levels. A. Representative images of BPGM, SynI and SynII expression and co-localization (arrows) in the placental labyrinth at E16.5. Scale bars: 5 µm. (**B**,**E**) Representative images and quantification of BPGM expression in the placental labyrinth at E16.5 of control and hypoxic chamber groups. Scale bars: 30 µm. (**C**,**D**,**F**) Trophoblast cells lining the arteries show an increase of BPGM expression in chronic hypoxia group. The expression of BPGM is restricted to the apical trophoblast cell side facing the arterial lumen. Scale bars: 30 µm. (C), 10 µm (D). Data are from 3 control, 4 chronic hypoxia and 4 acute hypoxia dams, 2-3 placentae per group and presented as mean ± SD values. Ordinary one-way ANOVA test was used for statistical analysis.

377 **Hypoxia Inducible Factor 1 Subunit Alpha (Hif1a) is Upregulated in Placental Cells Following**
378 **Acute Gestational Hypoxia**

379 Our present findings revealed upregulated expression of BPGM in placental cells following
380 gestational hypoxia. Hif1a is a transcription factor that plays an important role in placental
381 development and is upregulated following hypoxia. Moreover, murine BPGM has several
382 potential Hif1a binding sites (Figure 5 Figure supplement 1). Therefore, we inspected the
383 expression of Hif1a in the labyrinth of the gestational hypoxia FGR murine model compared to
384 the control. Significant differences were observed in the syncytiotrophoblast Hif1a expression
385 between the acute hypoxic and control placentae (Figure 5 A, B). Interestingly, no differences
386 were observed for the chronic placentae. In addition, we inspected Hif2a expression in the
387 labyrinth of the gestational hypoxia FGR murine model compared to the control, however no
388 significant differences were observed (Figure 5 C, D).

389

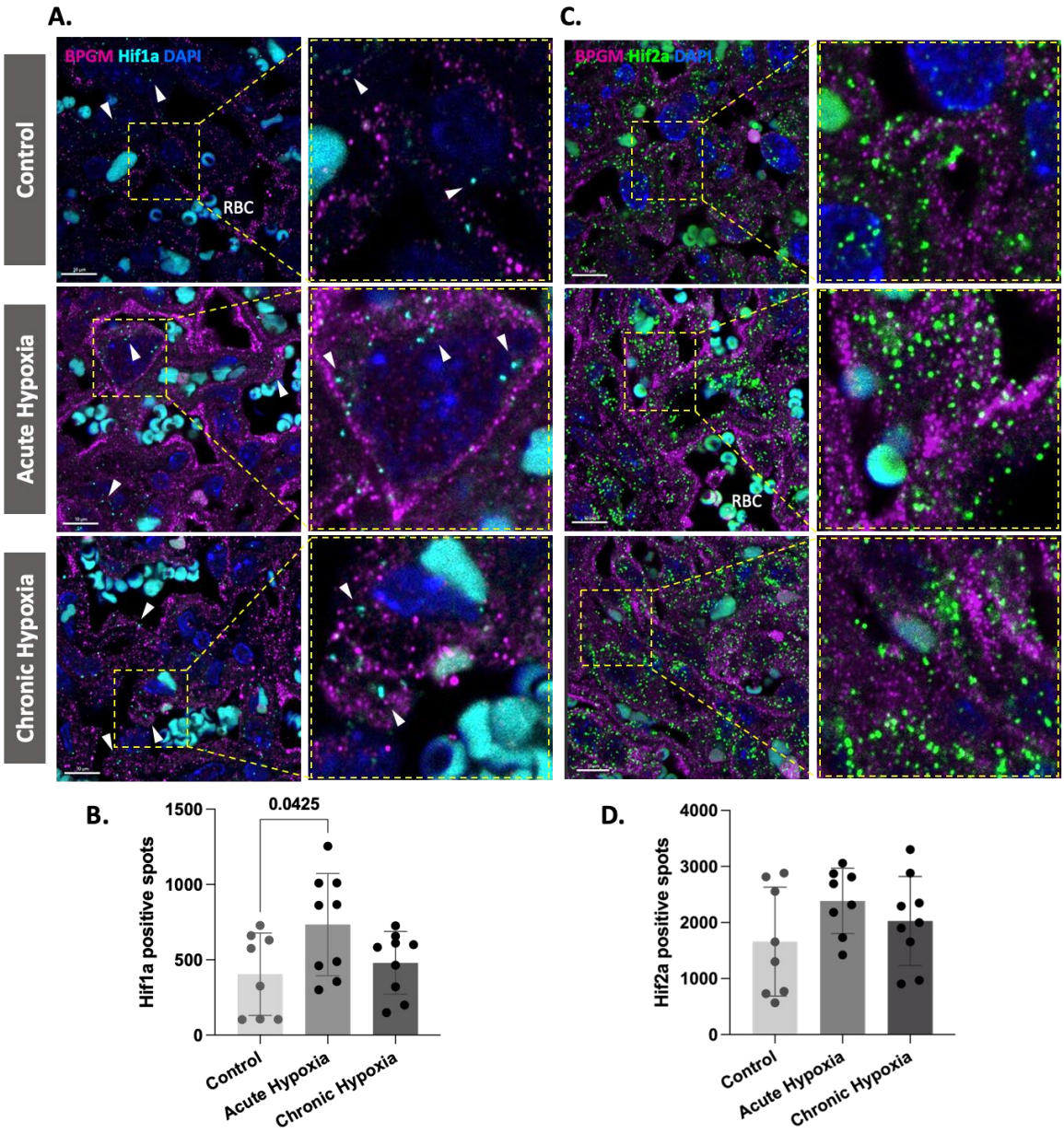

Figure 5. Hif1a is upregulated in acute hypoxic placentae. (**A**,**D**) Representative images and quantification of Hif1a and Hif2a expression in the placental labyrinth at E16.5 of control and hypoxic chamber groups. Scale bars: 10 µm (**A,C**). Data are from 2-3 placentae per group, each from different litter and presented as mean + SD values. Ordinary one-way ANOVA test was used for statistical analysis.

BPGM Expression is Downregulated in Human FGR Placentae

398 An upregulation of syncytiotrophoblast and SpA TGCs BPGM levels was detected in the murine
399 gestational hypoxia placentae. Therefore, to determine whether BPGM expression is also
400 altered in human placental syncytiotrophoblast cells of pregnancies complicated by FGR, human
401 placentae from healthy and FGR-complicated third-trimester pregnancies were examined.
402 Seventeen samples collected from Meir and Wolfson Medical Centers were selected from 236
403 deliveries, following childbirth and classified into two groups: FGR complicated pregnancies and
404 matched control deliveries (Table 1 and Figure 6). Clinical characteristics and neonatal outcomes
405 are provided in Table 1. Clinical parameters did not differ among the groups, except for
406 birthweight, which was significantly lower in the FGR group, as compared with the control
407 (Unpaired t-test; P = 0.0004). A downregulation of syncytiotrophoblast cells BPGM levels was
408 observed in the FGR placentae (Figure 7 A-C, Unpaired t-test, P= 0.0460). No differences were
409 observed in 2,3 BPG levels in maternal plasma analyzed by mass spectrometry (Figure 7 D, E).
410 However, the results demonstrated a significant reduction of 2,3 BPG levels in cord plasma from
411 FGR complicated pregnancies (Figure 7 D, F).

412

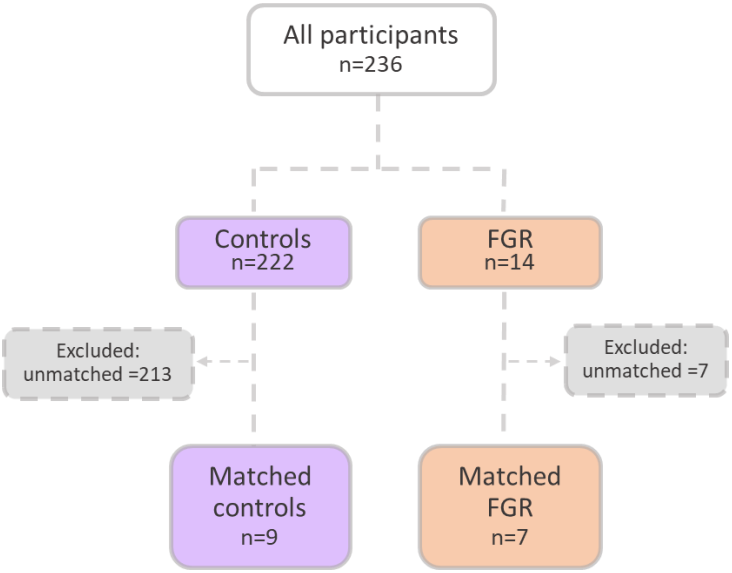

413

414 **Figure 6. Patient selection flow chart.** 16 Pregnant women were recruited from the Meir and
415 Wolfson Medical Centers.

416

Parameter	**Control** ***n*=9**	**FGR** ***n*=7**	***P* value**

Maternal age, mean ± SD, years	30.2 ± 5.6	29.14 ± 5.6	0.7291
Gestational age, mean ± SD, weeks	38.2 ± 1	37.5 ± 0.6	0.1644
Preterm delivery (<37), *n* (%)	0	0	
Pregravid BMI (kg/m^2), mean ± SD	22.8 ± 4.5	27.1 ± 3.6	0.2598
Gravidity, median (IQR)	2.3 (1.5)	2. (2)	
Parity, median (IQR)	1.2 (1.5)	1 (2)	
Maternal comorbidities, *n* (%)			
Hypertensive disorders	0	0	
Diabetes or gestational diabetes	1 (11)	1 (14)	
Asthma	0	0	
Thyroid disease	0	0	
Smoker	5	3	
Infant sex, *n* (%)			
Male	7 (77)	4 (57)	
Female	2 (23)	3 (43)	
Birthweight, mean ± SD, grams	3167 ± 494	2189.4 ± 189	***0.0004
NICU, *n* (%)	0	1 (14)	

Table 1. Clinical parameters of women included in the study. Clinical parameters did not differ among the groups, except for birthweight, which was significantly lower in the FGR group (Unpaired *t*-test, *P*=0.0004)**.**

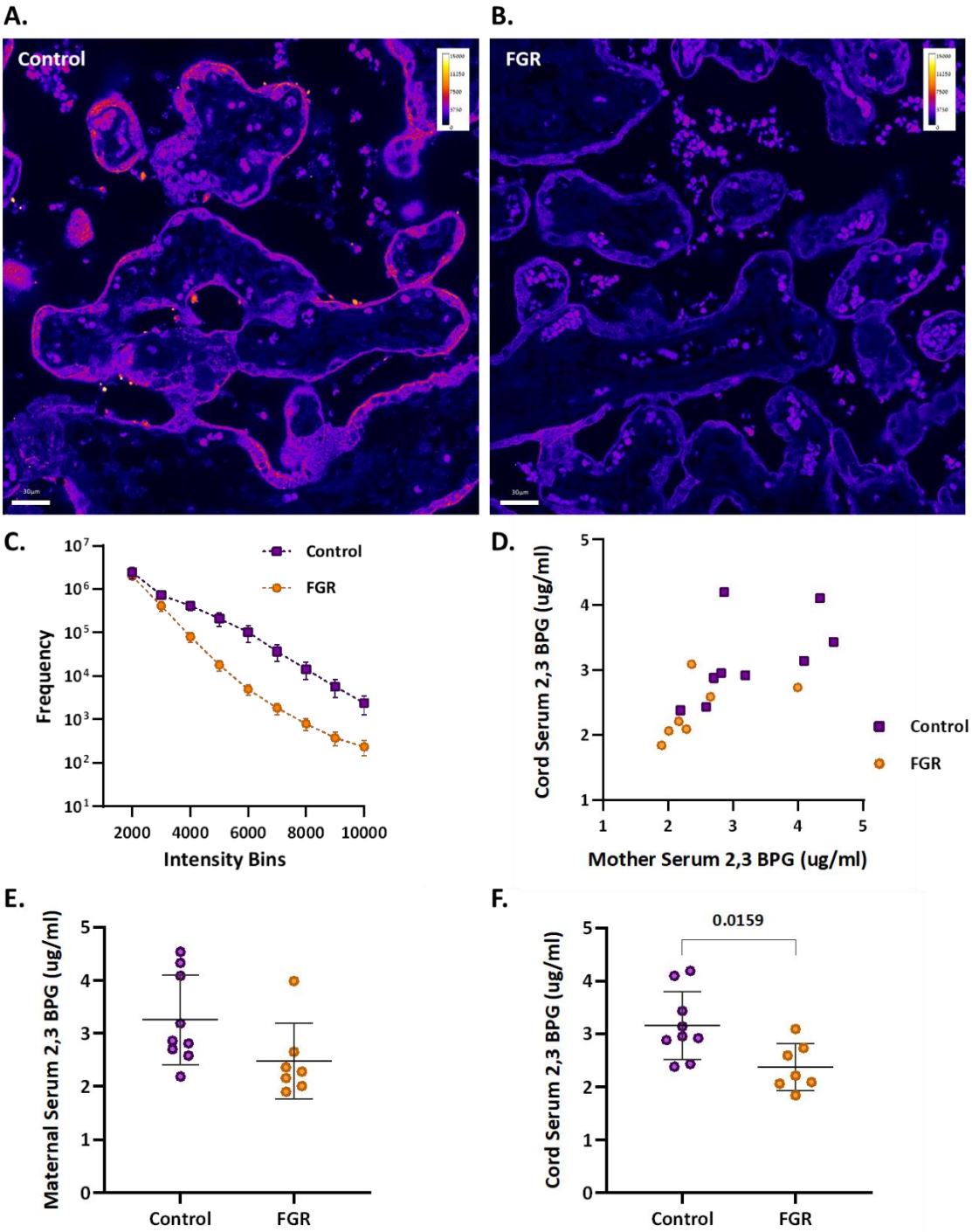

Figure 7. Human FGR placentae exhibit lower BPGM and 2,3 BPG levels. (**A, B**) Representative images of BPGM expression in control and FGR placentae. Scale bars: 30 µm. (**C**) Graph representing intensity of BPGM expression in control and FGR placentae. (**D-F**) Levels of 2,3 BPG in maternal and cord serum of control and FGR placentae. Data are from 9 control and 7 FGR women and presented as mean ± SD values. Unpaired *t* test was used for statistical analysis.

429 **Discussion**

430 Proper placental and fetal oxygenation is essential for a healthy pregnancy. Accordingly,
431 maternal gestational hypoxia constitutes a risk factor for FGR incidence[34]. However, the etiology
432 and molecular mechanism underlying idiopathic as well as maternal gestational hypoxia induced
433 FGR remains unclear. In order to elucidate on the mechanisms leading to FGR, this study
434 employed a murine FGR model based on maternal acute and chronic gestational hypoxia.
435 Hypoxia-induced FGR placentae displayed smaller labyrinth fraction, higher RBC content and
436 enlarged spiral arteries. However, *in vivo* functional MRI experiments in response to hypoxia-
437 hyperoxia challenge are consistent with similar deoxyhemoglobin content in all groups. Oxygen
438 release under hypoxia might be regulated by 2,3 BPG, as suggested by the BPGM expression in
439 the murine hypoxic placentae which was upregulated and concentrated in the cell side facing
440 the maternal circulation. The murine levels of placental Bpgm might be regulated via Hif1a, a
441 transcriptional regulator of cellular and developmental response to hypoxia. Conversely, human
442 FGR placentae of unknown etiology exhibited an opposite phenotype, presenting lower BPGM
443 expression and reduced level of 2,3 BPG in the cord serum. This suggests that induction of
444 placenta BPGM may be part of the hypoxic adaptation response in the murine placenta; while
445 suppression of BPGM may contribute to placenta deficiency in the human FGR.

446 Intra-uterine hypoxia has adverse effects on placental and embryonic development. This study
447 shows a decreased placental and embryonal weight, and a reduction in the percent of AGA and
448 LGA placentae and fetuses in the gestational hypoxia groups, with no difference in litter size
449 between hypoxic and control groups. Moreover, the labyrinth area of hypoxic placentae was
450 significantly smaller, implying an improper placental development. Previous studies showed that
451 intermittent hypoxia increased placental weight and labyrinth size, while chronic gestational
452 hypoxia in mice leads to reduced litter size and had no effect on the labyrinth zone[3536]. These
453 contradictory results may be due to the different experimental setups employed in the
454 intermittent hypoxia model, and the differences in litter size of the chronic hypoxia model,
455 which might in turn affect placental size and development. Furthermore, the current study
456 demonstrated an increase in the diameter of placental SpA following gestational hypoxia. This
457 enlargement might serve as a compensational mechanism for the placental and labyrinthine size
458 reduction, by supplying higher volumes of blood to the placenta thereby increasing oxygen
459 content, tissue oxygenation and oxygen supply to the fetus. Previous studies have shown that

460 gestational hypoxia from mid-late gestation increased the diameter of radial arteries compared
461 to control[15]; however, no significant difference was observed in the spiral arteries, possibly due
462 to the late exposure to hypoxia. However, this study mimics adaptation to early gestational
463 hypoxia and early onset placental dysfunction leading to severe FGR and therefore, might serve
464 as a better model for the human hypoxic-induced FGR.

465 MRI is an important tool for imaging changes in deoxyhemoglobin concentration *in vivo*.
466 Previous *in vivo* studies on non-treated pregnant mice obtained oxygen-hemoglobin dissociation
467 curves in mid-late gestation placentae under hyperoxia - hypoxia challenge[37]. Interestingly, in
468 the present study no significant differences were found in the R2* values between the hypoxic
469 and control placentae under hyperoxic, normoxic and hypoxic conditions. This result is
470 consistent with similar deoxyhemoglobin levels in the hypoxic and control placentae, despite the
471 upregulation of RBC levels in the hypoxic placentae. These results indicate that the partial
472 amount of HbO_2 is higher in the hypoxic placentae compared to the control, implying on the
473 ability of the placenta to maintain its oxygen levels albeit the maternal hypoxia.

474 In RBCs, the BPGM enzyme is responsible for the synthesis of 2,3 BPG, which induces the release
475 of oxygen from Hb in the mammalian organism. Remarkably, the expression of BPGM has been
476 reported in the human placental labyrinth[29], suggesting on its role in placental oxygen transfer.
477 This study shows for the first time the polar pattern of BPGM expression in both the murine and
478 human placental cells, amassing at the apical lumen, facing the maternal circulation. This polar
479 expression might increase the efficiency of oxygen sequestering from maternal blood by
480 reducing the distance between 2,3 BPG molecule and the maternal RBCs. Moreover, following
481 maternal intra-uterine hypoxia, the expression of murine placental BPGM is further upregulated,
482 suggesting a physiological role for placenta BPGM in the placental acclimatization to low oxygen
483 availability. Strikingly, attenuation in the expression of BPGM in FGR human placentae was
484 found when compared to the control. Moreover, 2,3 BPG levels in the cord serum of FGR
485 placentae were also decreased compared to control. This suggests that failure in induction of
486 placental BPGM and subsequently lower 2,3 BPG levels may contribute to the pathophysiology
487 of FGR. Remarkably, the same phenotype was observed in a murine FGR model of *igf2*+/-
488 knockout mice, where labyrinthine BPGM expression was lower compared to control dams[30].
489 This study demonstrates opposite BPGM expression patterns in mouse and human FGR,
490 suggesting that the murine FGR in our model originates in low maternal oxygen concentrations,

491 which are compensated by the placenta *via* upregulation of BPGM levels, while human FGR of
492 unknown etiology is related to a placental pathology that might include inadequate BPGM
493 expression. During human gestation, the γ hemoglobin subunit starts to decline around week 32
494 and β hemoglobin rises, switching from fetal to adult hemoglobin. Following this increase in HbA
495 in the fetus, it might be possible that placental BPGM and 2,3 BPG are also used by the fetus at
496 that stage, to mediate the release of oxygen to its organs. However, the question of how
497 placental 2,3 BPG might be transported to the nearby maternal RBCs needs to be addressed,
498 while a possible explanation would be a specific transport system. In summary, we hypothesize
499 that placental BPGM provides an important mechanism for placental adaptation to oxygen
500 transfer during the course of gestation. We propose that placental BPGM sequesters oxygen
501 from the maternal Hb, and facilitates oxygen diffusion from the maternal to the fetal circulation
502 (Figure 8). These results offer a possible causative link between the expression of this enzyme
503 and the development of an FGR. This novel molecular mechanism for the regulation of oxygen
504 availability by the placenta might provide a better understanding of the FGR pathology and
505 possibly pave the way toward development of novel therapies for FGR complications.

506 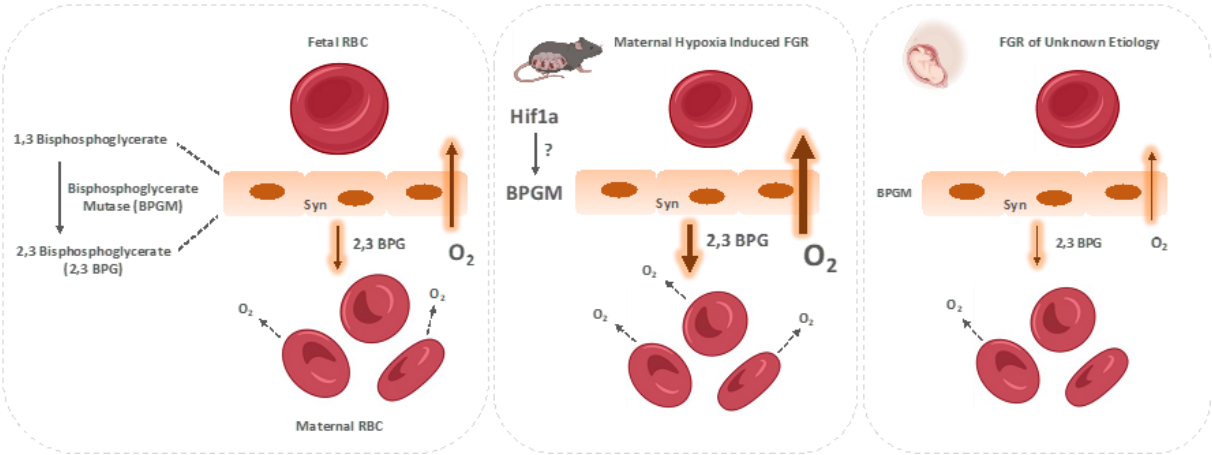

507 **Figure 8. Proposed model of placental adaptation to oxygen transfer during the course of**
508 **gestation.** Expression of BPGM, a key enzyme affecting the release of oxygen from hemoglobin,
509 is augmented in the murine placenta challenged by gestational hypoxia in mice, while its
510 expression is attenuated in placenta of human FGR. The placental upregulation of BPGM might
511 be mediated *via* Hif1a.

512

513 **Acknowledgements**

This work was supported by the Weizmann Krenter Foundation and the Weizmann – Ichilov (Tel Aviv Sourasky Medical Center) Collaborative Grant in Biomedical Research, and by the Minerva Foundation (to MN), by the ISF KillCorona grant 3777/19 (to MN, MK).

Conflict-of-Interest

The authors declare no conflicts of interest.

Data availability

Source data is available at https://www.ebi.ac.uk/biostudies/bioimages/studies/S-BIAD1030

References

1. Gude NM, Roberts CT, Kalionis B, King RG. Growth and function of the normal human placenta. *Thromb Res*. 2004;114(5-6 SPEC. ISS.):397-407. doi:10.1016/j.thromres.2004.06.038

2. Garnica AD, Chan WY. The role of the placenta in fetal nutrition and growth. *J Am Coll Nutr*. 1996;15(3):206-222. doi:10.1080/07315724.1996.10718591

3. Burton GJ, Fowden AL. The placenta: A multifaceted, transient organ. *Philos Trans R Soc B Biol Sci*. 2015;370(1663). doi:10.1098/RSTB.2014.0066

4. Woods L, Perez-Garcia V, Hemberger M. Regulation of Placental Development and Its Impact on Fetal Growth—New Insights From Mouse Models. *Front Endocrinol (Lausanne)*. Published online 2018. doi:10.3389/fendo.2018.00570

5. Sun C, Groom KM, Oyston C, Chamley LW, Clark AR, James JL. The placenta in fetal growth restriction: What is going wrong? *Placenta*. 2020;96:10-18. doi:10.1016/J.PLACENTA.2020.05.003

6. Romo A, Carceller R, Tobajas J. Intrauterine Growth Retardation (IUGR): Epidemiology and Etiology. *Abstr Ref Ped Endocrinol Rev*. 2008;6:pp.

7. Lausman A, Kingdom J, Gagnon R, et al. Intrauterine growth restriction: Screening, diagnosis, and management. *J Obstet Gynaecol Canada*. 2013;35(8):749-757. doi:10.1016/S1701-2163(15)30866-5

8. Sharma D, Shastri S, Sharma P. Intrauterine Growth Restriction: Antenatal and Postnatal Aspects. Clin Med Insights Pediatr. 2016;10:67. doi:10.4137/CMPED.S40070

9. Von Beckerath AK, Kollmann M, Rotky-Fast C, Karpf E, Lang U, Klaritsch P. Perinatal complications and long-term neurodevelopmental outcome of infants with intrauterine growth restriction. *Am J Obstet Gynecol*. 2013;208(2):130.e1-130.e6. doi:10.1016/J.AJOG.2012.11.014

10. Chew LC, Verma RP. Fetal Growth Restriction. In: StatPearls. Treasure Island (FL): StatPearls Publishing; June 11, 2022.

11. Ghidini A. Idiopathic fetal growth restriction: A pathophysiologic approach. *Obstet*

549 *Gynecol Surv*. 1996;51(6):376-382. doi:10.1097/00006254-199606000-00023

550 12. Burton GJ. Oxygen, the Janus gas; its effects on human placental development and
551 function. In: *Journal of Anatomy*. ; 2009. doi:10.1111/j.1469-7580.2008.00978.x

552 13. Carter AM. Placental gas exchange and the oxygen supply to the fetus. *Compr Physiol*.
553 Published online 2015. doi:10.1002/cphy.c140073

554 14. Zhou J, Xiao D, Hu Y, et al. Gestational hypoxia induces preeclampsia-like
555 symptoms via heightened endothelin-1 signaling in pregnant rats. *Hypertension*.
556 2013;62(3):599-607. doi:10.1161/HYPERTENSIONAHA.113.01449

557 15. Cahill LS, Rennie MY, Hoggarth J, et al. Feto- and utero-placental vascular adaptations to
558 chronic maternal hypoxia in the mouse. *J Physiol*. 2018;596(15):3285-3297.
559 doi:10.1113/JP274845

560 16. Higgins JS, Vaughan OR, Fernandez de Liger E, Fowden AL, Sferruzzi-Perri AN. Placental
561 phenotype and resource allocation to fetal growth are modified by the timing and degree
562 of hypoxia during mouse pregnancy. *J Physiol*. 2016;594(5):1341-1356.
563 doi:10.1113/JP271057

564 17. Tomlinson TM, Garbow JR, Anderson JR, Engelbach JA, Nelson DM, Sadovsky Y. Magnetic
565 resonance imaging of hypoxic injury to the murine placenta. Am J Physiol - Regul Integr
566 Comp Physiol. 2010;298(2):312-319. doi:10.1152/ajpregu.00425.2009

567 18. Howard RB, Hosokawa T, Maguire MH. Hypoxia-induced fetoplacental vasoconstriction in
568 perfused human placental cotyledons. *Am J Obstet Gynecol*. 1987;157(5):1261-1266.
569 doi:10.1016/S0002-9378(87)80307-1

570 19. Mairbäurl H, Weber RE. Oxygen Transport by Hemoglobin. Published online 2012.
571 doi:10.1002/cphy.c080113

572 20. Avni R, Neeman M, Garbow JR. Functional MRI of the placenta – From rodents to
573 humans. *Placenta*. 2015;36(6):615-622. doi:10.1016/J.PLACENTA.2015.04.003

574 21. Avni R, Golani O, Akselrod-Ballin A, et al. MR Imaging–derived Oxygen-Hemoglobin
575 Dissociation Curves and Fetal-Placental Oxygen-Hemoglobin Affinities. *Radiology*.
576 2016;280(1):68-77. doi:10.1148/radiol.2015150721

577 22. Sasaki R, Ikura K, Narita H, Yanagawa S ichi, Chiba H. 2,3-bisphosphoglycerate in
578 erythroid cells. *Trends Biochem Sci*. 1982;7(4):140-142. doi:10.1016/0968-
579 0004(82)90205-5

580 23. Mulquiney PJ, Kuchel PW. Model of 2,3-bisphosphoglycerate metabolism in the human
581 erythrocyte based on detailed enzyme kinetic equations: equations and parameter
582 refinement. Biochem J. 1999;342 Pt 3(Pt 3):581-596.

583 24. Steinberg MH, Benz EJ, Adewoye AH, Ebert BL. Pathobiology of the Human Erythrocyte
584 and Its Hemoglobins. *Hematol Basic Princ Pract*. Published online 2018:447-457.
585 doi:10.1016/B978-0-323-35762-3.00033-0

586 25. Bauer DE, Kamran SC, Orkin SH. Reawakening fetal hemoglobin: prospects for new
587 therapies for the-globin disorders. Published online 2012. doi:10.1182/blood

588 26. Bauer C, Ludwig I, Ludwig M. Different effects of 2.3 diphosphoglycerate and adenosine
589 triphosphate on the oxygen affinity of adult and foetal human haemoglobin. *Life Sci*.
590 1968;7(23):1339-1343. doi:10.1016/0024-3205(68)90249-X

591 27. Frier JA, Perutz MF. Structure of human foetal deoxyhaemoglobin. *J Mol Biol*.
592 1977;112(1):97-112. doi:10.1016/S0022-2836(77)80158-7

593 28. Adachi K, Konitzer P, Pang J, Reddy KS, Surrey S. Amino Acids Responsible for Decreased
594 2, 3-Biphosphosphoglycerate Binding to Fetal Hemoglobin. *Blood*. 1997;90(8):2916-2920.
595 doi:10.1182/BLOOD.V90.8.2916

596 29. Pritlove DC, Gu M, Boyd CAR, Randeva HS, Vatish M. Novel Placental Expression of 2,3-
597 Bisphosphoglycerate Mutase. *Placenta*. 2006;27(8):924-927.
598 doi:10.1016/j.placenta.2005.08.010

599 30. Gu M, Pritlove DC, Boyd CAR, Vatish M. Placental Expression of 2,3 Bisphosphoglycerate
600 Mutase in IGF-II Knock out Mouse: Correlation of Circulating Maternal 2,3
601 Bisphosphoglycerate and Fetal Growth. *Placenta*. 2009;30(10):919-922.
602 doi:10.1016/j.placenta.2009.08.005

603 31. Keyes LE, Armaza JF, Niermeyer S, Vargas E, Young DA, Moore LG. Intrauterine Growth
604 Restriction, Preeclampsia, and Intrauterine Mortality at High Altitude in Bolivia. *Pediatr*
605 *Res 2003 541*. 2003;54(1):20-25. doi:10.1203/01.pdr.0000069846.64389.dc

606 32. Jang EA, Longo LD, Goyal R. Antenatal maternal hypoxia: Criterion for fetal growth
607 restriction in rodents. *Front Physiol*. 2015;6(MAY):176.
608 doi:10.3389/FPHYS.2015.00176/BIBTEX

609 33. Faura J, Ramos J, Reynafarje C, English E, Finne P, Finch CA. Effect of Altitude on
610 Erythropoiesis. *Blood*. 1969;33(5):668-676. doi:10.1182/BLOOD.V33.5.668.668

611 34. Ducsay CA, Goyal R, Pearce WJ, Wilson S, Hu XQ, Zhang L. Gestational hypoxia and
612 developmental plasticity. Physiol Rev. 2018;98(3):1241-1334. doi:
613 10.1152/physrev.00043.2017

614 35. Matheson H, Veerbeek JHW, Charnock-Jones DS, Burton GJ, Yung HW. Morphological
615 and molecular changes in the murine placenta exposed to normobaric hypoxia
616 throughout pregnancy. *J Physiol*. 2016;594(5):1371-1388. doi:10.1113/JP271073

617 36. Badran M, Abuyassin B, Ayas N, Laher I. Intermittent hypoxia impairs uterine artery
618 function in pregnant mice. *J Physiol*. 2019;597(10):2639-2650. doi:10.1113/JP277775

619 37. Avni R, Golani O, Akselrod-Ballin A, et al. MR Imaging–derived Oxygen-Hemoglobin
620 Dissociation Curves and Fetal-Placental Oxygen-Hemoglobin Affinities. *Radiology*.
621 2016;000(0):150721. doi:10.1148/radiol.2015150721

622 38. Schindelin J, Arganda-Carreras I, Frise E, et al. Fiji: An open-source platform for biological-
623 image analysis. *Nat Methods*. 2012;9(7):676-682. doi:10.1038/NMETH.2019

624 39. Cartharius K, Frech K, Grote K, Klocke B, Haltmeier M, Klingenhoff A, Frisch M, Bayerlein
625 M, Werner T (2005) MatInspector and beyond: promoter analysis based on transcription factor
626 binding sites. Bioinformatics 21, 2933-42

627 **Supplementary**

628

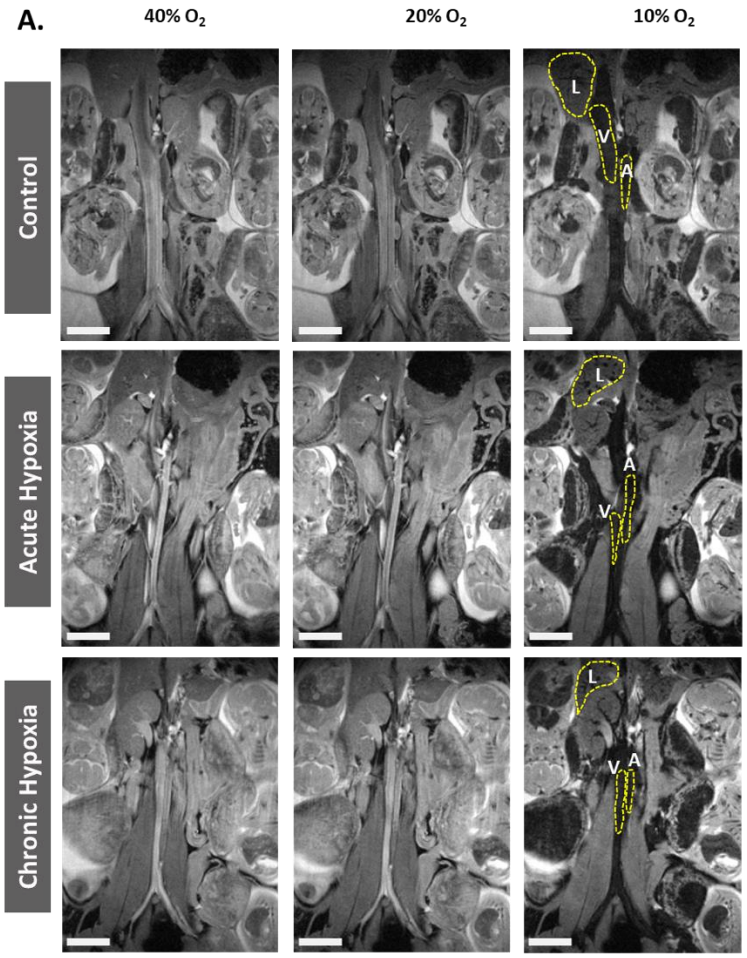

629

630 **Figure 3 Figure supplement 1. Effects of maternal hypoxia during gestation on R2* values**
631 **following hyperoxia-hypoxia challenge.** (**A**) Representative R2* images of control and hypoxic
632 chamber group show several dams and their liver (L), aorta (A) and vena cava (V). Scale bars: 0.5
633 cm.

634

635 **Figure 3 Supplementary video 1, 2, 3. MR imaging of mother, embryos and placentae:**
636 Representative MRI scan videos of control, acute and chronic hypoxia dams respectively.

637

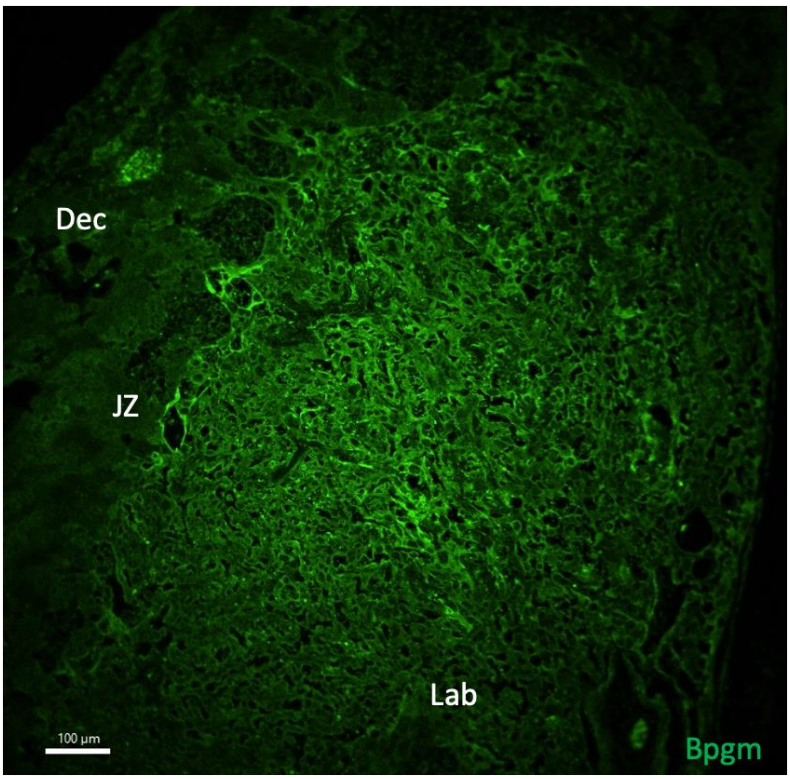

Figure 4 Figure supplement 1. BPGM expression in a control murine placenta. BPGM expression is restricted to the labyrinth area.

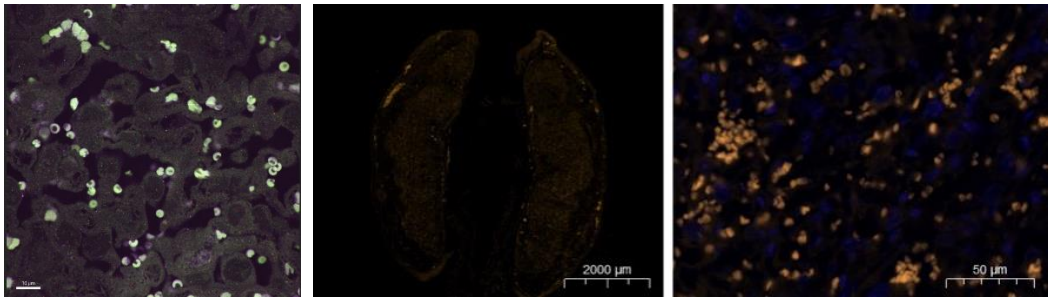

Figure 4 Figure supplement 2. Negative Controls for the BPGM IHC. The positive signal comes from the RBC auto fluorescence.

Figure 5 Figure supplement 1. Murine BPGM Promoter Analysis. Potential Hif1 binding sites.

V$HIFF = Hypoxia inducible factor family binding sites

Blue text = first exon

Red text = genomic repeat (from RepeatMasker)

Mouse GRCm38

650 >chr6:34474344-34477250
651 CATCTCTTCAGCCTTAGAATTAAATTCCTCATAGCTGGAATACATTGCTTGTGGGAGGTGGAGGCAGTTGTA
652 AGAAAAAAGGCTTTCCCCAGAACTATAAATTAGCAGCCTTGGGTTTTTGTTTCAATCCCCTATTGTTTGTGC
653 AAGGAACCAGGTAGGGTTCTTTCTAAGGCCCAGTGAAGTAAGGCGTAGTCTAATGTTTTTGAAGGTCATCTT
654 TGCCTCAAATGGATTTATGATAATCTTTGTGAGCACAGGTTCACTCTTTCAACGTTCTCAAGGCAAACAGCT
655 CACAGACAGATCGGAACATGGGGTCCAGGATATGATATTGCGATCTAGATAAACATAAGAACAATCTTGCCA
656 TGCAACAGTGACTCCTGCCATTGCTAACTTCTGTGAATACCTGTGTCGTAAAGACCAGGCTTGCTCCCAACA
657 CTCGCTTTCACATCCCACCTAAGAGCATCATAGGTAAAGATGTTTTGTTTTTTTTTAAAATAACAATGTACA
658 CACTAGTGACCCTGGTGAATAGTTCTAAAAGACAAGTATTGTAAAGTTTTATATGCCAAGCTAGTGTTATTG
659 AGTATTCCTAACAAGGTCAAAGTAAATCAAATGAGCAGGCATCCTAAGGTTCAGAGTACCCTCAAATGTCAA
660 ATGCTGTATGGCTGTTAGGATTGGTTTTGCATGGCTGCCGTTACCCTTCCTGAGGAGAAAGCTTTGATACTA
661 CAGGGCAGCGGAAATGTTTTCTGGTCCATCTGCCCTCATGAAGAAGAGGAAGAACAGGTTGGCAGGTGTGTA
662 CGATTGGGCAGATTCCTTCTCCAGCTGTTCTGACCTGAGAATCCACTGGCTAAGACAAGTAGCCACACCTGA
663 GCCATCCAGGAGGTAGAGTTTAACTTTGCTAAGCCACCATCACTACAGCACTGGGTTCACACACCATCACTC
664 CAGCCGACAGAACTCACTGTCCTTGAGAGACGCTCTCTCAGAAAGGGGTAGCTGCAACTATCATGAGCTAAA
665 ATGCATAAATGGGACATACAGCTTGCTACAAGCAGGCCATCATGACACCAGTTCATGGTGTGTCAAGATTTT
666 CATCCTAAATAACTGATCTGAGCACCCATTAGCTGGTCACAAACTTATTGGACTTGTTTATAGAATTAACTA
667 GGTGAGTTCAGAAGACACTAAGTGGAACAGCTTTCAGAAACCAAGAAGGGGAATTTTCCCGTCTGCTCAGGC
668 ACACATAACATTTCTTATCTTTCTCATTCACGTTTTGACACACGTTTCAGACCTTGTGTGGTAGTTCAAGCC
669 TGCTTAGTAGCTTCCAGCTCTGGTACCAGACCCGAGTGACAAGCTGGCATTTTCATAGGTTTAATTTCAGAA
670 ACTGTAGTGTACCATTTTCTACTTTTCTAACCTCTTCGCCCTTCTTGTACTTTTAGGATATCCTATTATTCG
671 CTTCTCTTCTCTTCATAATGTTAGGAGAAAGTAAGAATGAGCGACTATCTGTAAATAGGACACTTTAAAGGT
672 TTTCATTTTAATCTCTGTTTTCGACGCACAGGCGTGCCAAACAAGCTTTCGTGAGGATCTACCGGGTTCAGC
673 CTAGGTAGGACCTGAAATTTTCCGTTAACTAGAAGAAGTATCCCTTCATCTGCTGACCCGCTTTTCACAGCA
674 GGTGTGTTTCAATTTCGAGAACTTCAAACAGGTCTCTGGACGGCAAAGCTAGCAGCCCACAAACATTGCCCC
675 GGCGATGCTCAGGGGTTTGGGTCTCTACGACTAAAGCCCGCCTGCCTATGTCCGAAACTACCATCTTATTGG
676 TCTATCCGTGCGTCTGTTTCCTCATTAAACCAATCATAGCTTCCCTTCTTACCCCAGGGACTTGAGAAACCG
677 GAAAGAACCTCCGGCTGGTCGCTGGCCAGAGGGCGGGGCCGTGAATGAGTGACAACTCTGTCTTCCAATACC
678 CAGCGCTATCGGTTCTGACCATTTTGGCTTCTAGGCTACAAAAGAGCGTTGATGCCGGCTGTAGCGATgaat
679 cctcactggcgtctgcagcacggcgttaccgaggaccggctgctactggtagtttccttgcagGTGAGTGGC
680 TTCGTTGTAATTGTTACAGTTGTGAGGATTTCTTTTCTTTCATGAGTGGCTTGCTGTTCTATCGTGAGAAGG
681 CCGGTTGCTACCTTGCCCGGCTTTAGTATCTGGTGGGAACCTGATGCCCGCTTCAAGCGAGACCCTCCCGAG
682 TACCCCAGCTCTCAGCTGGCCCTTTCTCAGCGAGCATCTCTCAGGAACAGTGAGTTCTGTCGGCTGGAGTGA
683 TGGTGTGTGAACCCAGAGCTGTAGTGATGGTGGCTTAGCAAAGTTAAACTCTACCTCCTGGATAGCTCAGGT
684 GTGGCTACTTGTCTTAGCCAGTGGATTCACTGGAAGGAAGCAGGTGTAGGGCGAAGGCAGACCTTGATCCTA
685 AAAGTGTAAGTTAAGGGGGGAAATATCATGGAAGGCAAAGAGGTTGTTGCATATTCAGGAGTCTCAGGAACC
686 ATATTCCGGGTTCAGGGGAACACTACCCCCTCCCCAGCACACACGCGTGCACGCCCGACCACCACTATCATG
687 GCCAAAAAGTGTCATTTCTTTTTGTGCTAAGGGGTAGGAGCAAGTATTTCACTACAGTAAGTCAAAAGAAAT
688 GCAAAATTGTAATGAAGTTTATTATTAGACTTTGCAGGATGGAGCCCCCCCCCCCAAATTAGGAAGGGTTTA
689 TAGCCCGTGAATGGGGGAAATGGTTCTAGAATATTAACTAACAGAATTCCGACGCCTTCGGGAGGAAATAAA
690 AAGTAAATGGTTACATTTCAGCAGCAGGTACAAACGTTTCTATAATAAAAGTCGTGTTAGTTTGTCTGTAAA
691 ACTGAATTTTCACATTTTTTTAAAAGA

692